

Rotating Bose gas with hard-core repulsion in a quasi-2D harmonic trap: vortices in BEC

M. A. H. Ahsan and N. Kumar

Raman Research Institute, Sir C. V. Raman Avenue, Bangalore 560080, India.

We consider a gas of $N (= 6, 10, 15)$ Bose particles with hard-core repulsion, contained in a quasi-2D harmonic trap and subjected to an overall angular velocity Ω about the z -axis. Exact diagonalization of the $n \times n$ many-body Hamiltonian matrix in given subspaces of the total (quantized) angular momentum L_z , with $n \sim 10^5$ (e.g. for $L_z = N = 15$, $n = 240782$) was carried out using Davidson's algorithm. The many-body variational ground state wavefunction, as also the corresponding energy and the reduced one-particle density-matrix $\rho(\mathbf{r}, \mathbf{r}') = \sum_{\mu} \lambda_{\mu} \chi_{\mu}^*(\mathbf{r}) \chi_{\mu}(\mathbf{r}')$ were calculated. With the usual identification of Ω as the Lagrange multiplier associated with L_z for a rotating system, the $L_z - \Omega$ phase diagram (or the stability line) was determined that gave a number of critical angular velocities Ω_{ci} , $i = 1, 2, 3, \dots$, at which the ground state angular momentum and the associated condensate fraction, given by the largest eigenvalue of the reduced one-particle density-matrix, undergo abrupt jumps. A number of (total) angular momentum states were found to be stable at successively higher critical angular velocities Ω_{ci} , $i = 1, 2, 3, \dots$ for a given N . All the states in the regime $N > L_z > 0$ are metastable. For $L_z > N$, the L_z values for the stable ground states generally increased with the increasing critical angular velocities Ω_{ci} , and the condensate was strongly depleted. The critical Ω_{ci} values, however, decreased with increasing interaction strength as well as the particle number, and were systematically greater than the non-variational Yrast-state values for the single vortex state with $L_z = N$. We have also observed that the condensate fraction for the single vortex state (as also for the higher vortex states) did not change significantly even as the 2-body interaction strength was varied over several (~ 4) orders of magnitude in the moderately to the weakly interacting regime.

PACS numbers: 05.30.Jp, 67.40.-w, 03.75.Fi

I. INTRODUCTION

The experimental realization of Bose-Einstein Condensation (BEC) in dilute vapors of ultra-cold (nanokelvin) alkali atoms^{1–3}, and other systems⁴, trapped in harmonic potential wells has qualitatively extended the domain of occurrence of the quantum fluids^{5–7}. Unlike their dense and strongly interacting homogeneous (bulk) counterparts, e.g. liquid ⁴He, these mesoscopic gaseous systems are dilute, weakly or moderately interacting and inhomogeneous—with controllable density, effective dimensionality, and tunable atom-atom interactions of either sign⁸. Further, the creation^{10,9} of the vortex states with quantized circulation in externally rotated traps, as also the direct observation of phase coherence effects¹¹, has clearly revealed the phase rigidity characteristic of superfluidity associated with the BEC. The BEC in a weakly and repulsively interacting dilute Bose gas (*i.e.* with the s-wave scattering length $a_{sc} \ll$ the mean inter-atomic spacing and with the number of atoms in the condensate $N \gg 1$) has often been described macroscopically through the Gross-Pitaevskii equation based on the condensate amplitude as a slowly varying order-parameter⁶. Microscopic treatments going beyond the meanfield approximation and based on the many-body variational wavefunctions also exist, but involve heavy computations^{12,13} even for modest size of the system ($N \sim 10 - 50$). Besides, these many-body calculations have involved only the “Lowest Landau Level (LLL)” single-particle orbitals, with only the positive sign (with respect to the trap angular velocity $\Omega \hat{e}_z$) of the single-particle angular momentum quantum number m . The inter-atomic repulsion is known to qualitatively change the ground state properties of a system of weakly interacting neutral Bose gas (confined in a rotating harmonic trap) at $T=0$ in two distinct ways⁶. First, it leads to a depletion of the condensate fraction, which is equal to 1 for an ideal (non-interacting) Bose gas. Second, it gives a phase rigidity, or stiffness, to the ground state many-body wavefunction. This is responsible for the superfluid flow that manifests in the successive appearance of vortices with higher quantized circulations beyond certain critical angular velocities Ω_{ci} of the rotating trap. Both these aspects are well described by the one-particle reduced density-matrix $\rho_1(\mathbf{r}, \mathbf{r}')$ obtained from the N -body ground-state wavefunction $\Psi_0(\mathbf{r}_1, \dots, \mathbf{r}_N)$ by partial integration, or tracing out of the $N-1$ co-ordinates from the N -body pure density-matrix $\Psi_0^*(\mathbf{r}_1, \dots, \mathbf{r}_N) \Psi_0(\mathbf{r}'_1, \dots, \mathbf{r}'_N)$. (It is to be recalled in passing here that the condensate and the superfluid fractions are not the same thing. More specifically, e.g., for the non-rotating ground state, the condensate fraction is generally less than unity while the superfluid fraction, that includes the condensate as well as the above-the-condensate fraction, is exactly equal to unity. However, both the condensate as well as the superfluid fractions are characterized by the same quantum-mechanical phase whose gradient gives the superfluid velocity. Also, both vanish together above the critical temperature T_c . In fact, it is

the condensate that amplifies the effect of even the weakest repulsive interaction leading to absence of single-particle excitation and giving rise to the phase rigidity).

In this work, we have studied the effect of the 2-body repulsive interaction on the condensate fraction, and on the the critical angular velocities(Ω_{ci} , $i = 0, 1, 2, \dots$) for the appearance of different vortex states for a quasi-2D Bose gas confined in a highly anisotropic harmonic trap (with $\omega_z \gg \omega_{\perp}$) which is subjected to an overall rotation Ω about the z-axis. To this end we use a variational approach and calculate the ground state energy, the ground state wavefunction and the associated one-particle reduced density-matrix for different values of the interaction, in given subspaces of the total quantized angular momentum L_z . The many-body variational ground state wavefunction is obtained through the exact diagonalization of the $N \times N$ many-body Hamiltonian matrix with, e.g., $N = 240782$ for $L_z = N = 15$, using Davidson's algorithm. A distinctive feature of the present work is that in constructing the many-body variational ground state wavefunction for a given L_z (\equiv the eigenvalue corresponding to the z-component of the total angular momentum operator \hat{L}_z), we have included, in the configuration interaction, the one-particle states with the single-particle angular momentum ($\equiv \hat{l}_z$) quantum number m of *either* sign, as also the higher "Landau-Level(LL)" states. One of our main results is the variation of the critical angular velocities Ω_{c1} with the interaction strength $\Lambda_2 \equiv (N-1) \sqrt{\frac{2}{\pi} \frac{a_{sc}}{a_z}}$ (the meanings of various symbols will be given in the next section), namely, that not only does Ω_{c1} decrease with increasing Λ_2 , it also stays systematically higher than its non-variational value, e.g., that given by the relation $\Omega_{c1} = \omega_{\perp} (1 - \frac{\Lambda_2}{4})$ for the weakly interacting, dilute case^{14,13,15}. We have also observed that the condensate fraction for the single vortex state with $L_z = N$ (as also for the higher vortex states) does not change significantly even if the 2-body scattering length a_{sc} is changed over ~ 4 orders of magnitude in the moderately to the weakly interacting regime, namely, from $a_{sc} = 1000a_0$ to $1a_0$, where a_0 is the Bohr radius.

This paper is organized as follows. In Section 2, we begin with a more general system to bring out, in passing, the mathematical analogy between the system under study here and the other well known systems like in the Landau-Darwin-Fock problem and argue that in a certain limiting case of interest to us here, it becomes essential to go beyond the Lowest Landau Level(LL) approximation so as to include higher LLs and with the single-particle angular momentum eigenvalue m taking both positive as well as negative values in constructing the many-body basis functions. Section 3 describes briefly the construction of the many-body basis functions and the determination of the variational ground state wavefunction by diagonalizing the many-body Hamiltonian matrix using Davidson's algorithm. In Section 4, we outline the procedure for determining the critical angular velocities for the entry of the vortices into the system, and the determination of various density profiles obtained from the one-particle reduced density-matrix characterizing the vortical state. Finally, in Section 5, we present and discuss our results, and end the paper with a brief conclusion.

II. THE SYSTEM AND THE HAMILTONIAN

We begin by considering the general case of a system of interacting, spinless, charged particles (bosons) confined in an external harmonic potential(trap). The 2-body interaction potential is, however, assumed to be gaussian in the particle-particle separation. The trap is also subjected to an externally impressed rotation at an angular velocity $\Omega \equiv \Omega \hat{z}$, and to a uniform magnetic field $\mathbf{B} \equiv B \hat{z}$. The Hamiltonian for the system in a frame co-rotating with the angular velocity Ω is then

$$\begin{aligned} \hat{\mathbf{H}}^{rot} &= \hat{\mathbf{H}}^{lab} - \boldsymbol{\Omega} \cdot \hat{\mathbf{L}}^{lab} \\ \hat{\mathbf{H}}^{lab} &= \sum_{i=1}^N \left[\frac{1}{2m} \left(\frac{\hbar}{i} \nabla_i - q \mathbf{A}(\mathbf{r}_i) \right)^2 + \frac{1}{2} m \omega_{\perp}^2 (r_{\perp i}^2 + \lambda_z^2 z_i^2) \right] + \\ &\quad \frac{1}{2} \cdot \frac{4\pi\hbar^2 a_{sc}}{m} \cdot \left(\frac{1}{\sqrt{2\pi}\sigma} \right)^3 \sum_{i \neq j} \exp^{-\frac{1}{2\sigma^2} \{(r_{\perp i} - r_{\perp j})^2 + (z_i - z_j)^2\}} \end{aligned} \quad (1)$$

$$\text{with } \hat{\mathbf{L}}_z^{lab} = \sum_{i=1}^N \hat{\mathbf{l}}_z^{lab} = \frac{\hbar}{i} \sum_{i=1}^N (\mathbf{r}_i \times \nabla_i)_z, \quad \mathbf{B} = \nabla \times \mathbf{A} \quad \text{and} \quad \mathbf{A} \equiv \frac{\mathbf{B}}{2} (\hat{e}_z \times \mathbf{r}).$$

Here q is the charge of the particles and $\mathbf{A}(\mathbf{r}) \equiv \frac{\mathbf{B}}{2} (x\hat{e}_y - y\hat{e}_x)$ is the electromagnetic vector potential in the symmetric gauge. The co-ordinates $\{\mathbf{r}_i\}$ and the corresponding canonical momenta $\{\frac{\hbar}{i} \nabla_i\}$ refer to the laboratory frame. From now onwards, we will drop the superscript *lab* on the Hamiltonian $\hat{\mathbf{H}}^{lab}$, the total angular momentum $\hat{\mathbf{L}}_z^{lab}$, the single-particle angular momentum $\hat{\mathbf{l}}_z^{lab}$ and their respective eigenvalues, and these will always be assumed to refer to the

laboratory frame unless otherwise specified.

We now make the following assumptions. The confining asymmetric harmonic potential is highly oblate spheroidal, with $\lambda_z \equiv \frac{\omega_z}{\omega_{\perp}} \gg 1$, and hence our confined system is effectively quasi-2D with the x-y rotational symmetry; the repulsive 2-body scattering is dominantly in the s-wave channel with a scattering length a_{sc} and $\frac{4\pi\hbar^2 a_{sc}}{m}$ having the dimension of Energy \times Volume. The range σ of the 2-body interaction is small enough compared to the inter-atomic spacing so as to effectively give a δ -function interaction potential $V(\mathbf{r}, \mathbf{r}') = \frac{4\pi\hbar^2 a_{sc}}{m} \delta(\mathbf{r} - \mathbf{r}')$.

Now, for our N-body variational calculation we need to construct the N-body basis-functions with proper symmetry. Since the system above is rotationally invariant in the x-y plane, the z-component of the total angular momentum (L_z) is a good quantum number leading to block diagonalization of the Hamiltonian matrix into the subspaces of \hat{L}_z . The N-body basis-functions are, in turn, constructed as linear combinations of the symmetrized products of a finite number of single-particle basis-functions, which are chosen to be eigenfunctions of the unperturbed single-particle Hamiltonian. With this in mind, let us consider the non-interacting single-particle Hamiltonian $\hat{\mathbf{h}}$ in the rotating frame, which we now separate into the z and the (x-y)-plane (commuting) components, $\hat{\mathbf{h}}_z$ and $\hat{\mathbf{h}}_{\perp}$ respectively:

$$\begin{aligned} \hat{\mathbf{h}} = & \underbrace{\frac{1}{2m} \left(\frac{\hbar}{i} \nabla_{\perp} - q \frac{1}{2} (\mathbf{B} \times \mathbf{r}_{\perp}) \right)^2 + \frac{1}{2} m \omega_{\perp}^2 r_{\perp}^2 - \frac{\hbar}{i} \boldsymbol{\Omega} \cdot (\mathbf{r}_{\perp} \times \nabla_{\perp})}_{\mathbf{h}_{\perp}} \\ & + \underbrace{\frac{1}{2m} \left(\frac{\hbar}{i} \nabla_z \right)^2 + \frac{1}{2} m \omega_z^2 z^2}_{\mathbf{h}_z} \equiv \mathbf{h}_{\perp} + \mathbf{h}_z. \end{aligned} \quad (2)$$

The eigensolutions for $\hat{\mathbf{h}}_z$ are then given by

$$\begin{aligned} \hat{\mathbf{h}}_z \mathbf{u}_{n_z}(z) &= \epsilon_{n_z} \mathbf{u}_{n_z}(z), \quad \text{where} \quad \epsilon_{n_z} = \left(n_z + \frac{1}{2} \right) \hbar \omega_z, \quad n_z = 0, 1, 2, \dots, \\ \mathbf{u}_{n_z}(z) &= \sqrt{\frac{\alpha_z}{\sqrt{\pi} 2^{n_z} n_z!}} e^{-\frac{1}{2} \alpha_z^2 z^2} H_{n_z}(\alpha_z z), \\ \text{and} \quad \alpha_z &= \sqrt{\frac{m \omega_z}{\hbar}} \equiv \text{inverse of the longitudinal oscillator length (a}_z\text{)} \end{aligned}$$

Here H_{n_z} is the Hermite polynomial. We assume the system to be quasi-2D in that there is practically no excitation along the relatively stiffer z-axis, and hence we set $n_z = 0$.

Let us now consider $\hat{\mathbf{h}}_{\perp}$. Using $\boldsymbol{\Omega} = \Omega \hat{e}_z$, $\mathbf{B} = B \hat{e}_z$ and $\mathbf{r}_{\perp} = x \hat{e}_x + y \hat{e}_y$, we re-write it more explicitly as

$$\begin{aligned} \hat{\mathbf{h}}_{\perp} &\equiv -\frac{\hbar^2}{2m} \underbrace{\left[\frac{1}{r_{\perp}} \frac{\partial}{\partial r_{\perp}} \left(r_{\perp} \frac{\partial}{\partial r_{\perp}} \right) + \frac{1}{r_{\perp}^2} \frac{\partial^2}{\partial \phi^2} \right]}_{\hat{\mathcal{K}}_{\perp}} + \frac{1}{2} m \zeta_{\perp}^2 r_{\perp}^2 - \varsigma \hat{l}_z \equiv \hat{\mathcal{K}}_{\perp} - \varsigma \hat{l}_z \quad (3) \\ \text{with} \quad \zeta_{\perp} &\equiv \sqrt{\left(\frac{qB}{2m} \right)^2 + \omega_{\perp}^2}, \quad \text{the frequency for the harmonic confinement in the x-y-plane,} \\ \text{and} \quad \varsigma &\equiv \left(\frac{qB}{2m} + \Omega \right), \quad \text{the cyclotron-rotational(or the centrifugal) angular velocity} \\ &\quad \text{about the z-axis.} \end{aligned}$$

Here $\hat{\mathcal{K}}_{\perp}$ is the single-particle 2D-harmonic oscillator Hamiltonian, for which the eigensolutions are known to be:

$$\begin{aligned} \hat{\mathcal{K}}_{\perp} \mathbf{u}_{n,m}(r_{\perp}, \phi) &= \epsilon_{n,m} \mathbf{u}_{n,m}(r_{\perp}, \phi), \quad \hat{l}_z \mathbf{u}_{n,m}(r_{\perp}, \phi) = m \hbar \mathbf{u}_{n,m}(r_{\perp}, \phi), \\ \text{with} \quad \mathbf{u}_{n,m}(r_{\perp}, \phi) &= \sqrt{\frac{\alpha_{\perp}^2}{\pi} \cdot \frac{\left(\frac{1}{2} [n - |m|] \right)!}{\left(\frac{1}{2} [n + |m|] \right)!}} (r_{\perp} \alpha_{\perp})^{|m|} e^{-\frac{1}{2} \alpha_{\perp}^2 r_{\perp}^2} e^{im\phi} L_{\frac{1}{2}(n-|m|)}^{|m|}(\alpha_{\perp}^2 r_{\perp}^2), \\ \text{where} \quad \alpha_{\perp} &= \sqrt{\frac{m \zeta_{\perp}}{\hbar}} \equiv \text{the inverse of the transverse oscillator length (a}_{\perp}\text{)}, \\ \text{and} \quad \epsilon_{n,m} &= \left(\underbrace{2n_r + |m| + 1}_{n} \right) \hbar \zeta_{\perp} \equiv (n + 1) \hbar \zeta_{\perp}, \end{aligned}$$

$$\begin{aligned} \text{with } n_r &= 0, 1, 2, \dots, \quad m = -\infty, \dots, -1, 0, +1, \dots, +\infty, \\ \text{or equivalently, } n &= 0, 1, 2, \dots, \quad m = +n, +n-2, \dots, -n+2, -n. \end{aligned} \quad (4)$$

Here $L_{\frac{1}{2}(n-|m|)}^{[m]}(\alpha_{\perp}^2 r_{\perp}^2)$ ($\alpha_{\perp}^2 r_{\perp}^2$) is the Associated Laguerre polynomial. It may be noted in passing that the above Hamiltonian represents the well known Landau-Darwin-Fock^{16,17} problem in which ζ_{\perp} is the frequency for the harmonic confining potential in the x-y plane and ς is the cyclotron-rotational (centrifugal) angular velocity about the z-axis. Limiting to $n_r = 0$ and taking $m = 0, +1, +2, +3, \dots$, corresponds to the “Lowest-Landau Level(LLL)” approximation.

Let us examine the centrifugal/mechanical stability of the above system by re-writing $\hat{\mathbf{h}}_{\perp}$ as

$$\begin{aligned} \hat{\mathbf{h}}_{\perp} &= \underbrace{\frac{1}{2m} \left(\frac{\hbar}{i} \nabla_{\perp} - q \frac{1}{2} (\mathbf{B} \times \mathbf{r}_{\perp}) - m (\Omega \times \mathbf{r}_{\perp}) \right)^2}_{\hat{\mathcal{T}}} \\ &+ \underbrace{\frac{1}{2} m \omega_{\perp}^2 r_{\perp}^2 - \frac{1}{2} m (\Omega \times \mathbf{r}_{\perp})^2 - q \frac{1}{2} (\mathbf{B} \times \mathbf{r}_{\perp}) \cdot (\Omega \times \mathbf{r}_{\perp})}_{\hat{\mathcal{U}}} \equiv \hat{\mathcal{T}} + \hat{\mathcal{U}} \end{aligned}$$

Here $\hat{\mathcal{T}}$ is clearly a positive-definite operator. It can readily be shown that $\hat{\mathcal{U}}$ is negative-definite, null or positive definite according as $(\zeta_{\perp} + \varsigma)(\zeta_{\perp} - \varsigma)$ is negative, zero or positive, respectively.

For $\hat{\mathcal{U}}$ negative-definite, the Hamiltonian $\hat{\mathbf{h}}_{\perp} \equiv \hat{\mathcal{T}} + \hat{\mathcal{U}}$ is unbounded from below and there are no stable solutions. In the simpler case of vanishing magnetic field $\mathbf{B}=0$, this situation arises for $\omega_{\perp} < \Omega$, i.e, when the rotational angular velocity Ω becomes larger than the confining harmonic trap frequency ω_{\perp} .

For the special case of $\hat{\mathcal{U}}$ null, we have $\zeta_{\perp} = \varsigma$ and the Hamiltonian reduces to $\hat{\mathbf{h}}_{\perp} = \mathcal{K}_{\perp} - \zeta_{\perp} \hat{l}_z$. This gives rise to a situation analogous to the Landau problem when the frequency for the harmonic confinement is equal to the centrifugal frequency. Setting $\zeta_{\perp} = \frac{1}{2}\omega_c$, we have the eigenvalue equation

$$\begin{aligned} \hat{\mathbf{h}}_{\perp} \mathbf{u}_{n,m}(r_{\perp}, \phi) &= (\hat{\mathcal{K}}_{\perp} - \zeta_{\perp} \hat{l}_z) \mathbf{u}_{n,m}(r_{\perp}, \phi) = (\epsilon_{n,m} - m\hbar\zeta_{\perp}) \mathbf{u}_{n,m}(r_{\perp}, \phi) \\ \text{with } (\epsilon_{n,m} - m\hbar\zeta_{\perp}) &= \left(\underbrace{n_r + \frac{1}{2}(|m| - m)}_{\mathcal{N}} + \frac{1}{2} \right) \hbar\omega_c \equiv \left(\mathcal{N} + \frac{1}{2} \right) \hbar\omega_c \end{aligned}$$

where $n_r = 0, 1, 2, 3, \dots$, and $m = -\infty, \dots, -2, -1, 0, +1, +2, \dots, +\infty$;
or equivalently $\mathcal{N} = 0, 1, 2, 3, \dots$,
and $m = -\mathcal{N}, -(\mathcal{N} - 1), \dots, -2, -1, 0, +1, +2, \dots, +\infty$. (5)

Each of the \mathcal{N} levels, the so-called Landau Levels(LL), is infinitely degenerate corresponding to the infinitely many possible values of m . It is clear from the ordering of the single-particle energy levels (without interaction) in equation (5) that the single-particle states with positive m values (i.e those with the angular momentum parallel to the overall rotational angular velocity $\varsigma \equiv \varsigma \hat{e}_z$) are energetically favored. These states constitute a massively degenerate manifold. This is the usual rationale for using the positive m values only, in constructing the variational wavefunction for the Landau-like problem. This degeneracy for the special case of $\zeta_{\perp} = \varsigma$ is, however, lifted by the inter-particle interactions.

Finally, we consider the physically interesting case of $\hat{\mathcal{U}}$ positive-definite. The single-particle non-interacting Hamiltonian $\hat{\mathbf{h}}_{\perp}$, now becomes $\hat{\mathbf{h}}_{\perp} = \mathcal{K}_{\perp} - \varsigma \hat{l}_z$ with the eigenvalue solution:

$$\begin{aligned} \hat{\mathbf{h}}_{\perp} \mathbf{u}_{n,m}(r_{\perp}, \phi) &= (\hat{\mathcal{K}}_{\perp} - \varsigma \hat{l}_z) \mathbf{u}_{n,m}(r_{\perp}, \phi) = (\epsilon_{n,m} - m\hbar\varsigma) \mathbf{u}_{n,m}(r_{\perp}, \phi) \\ (\epsilon_{n,m} - m\hbar\varsigma) &= 2 \left(n_r + \frac{1}{2} \left(|m| - m \frac{\varsigma}{\zeta_{\perp}} \right) + \frac{1}{2} \right) \hbar\zeta_{\perp}, \end{aligned}$$

where $n_r = 0, 1, 2, \dots$, and $m = -\infty, \dots, -2, -1, 0, +1, +2, \dots, +\infty$. (6)

In this physically relevant situation, the particle as observed in the rotating frame finds itself in a shallower harmonic potential of frequency $\sqrt{\zeta_{\perp}^2 - \varsigma^2}$, and the states will be more spread out. It can be seen from equation(6) that for the centrifugal frequency ς significantly smaller than the confining frequency ζ_{\perp} , the degeneracy of the Landau levels is lifted even without interaction. Further, the interaction between the particles causes the the different single-particle

angular momentum states to scatter into each other. Thus, for the slowly rotating systems and for moderately, and a fortiori for strongly interacting systems, it may be necessary to include single-particle basis functions with different values of n_r and with the angular momentum quantum number m taking both positive and negative values. This is the case we shall be concerned with in the following with $B=0$ and $q=0$.

III. THE MANY-BODY VARIATIONAL WAVEFUNCTION

We need to perform the diagonalization of the Hamiltonian matrix in the subspaces of $\hat{\mathbf{L}}_z$ only. The N-body variational wavefunction $\Psi(\mathbf{r}_1, \dots, \mathbf{r}_N)$ is a linear combination of the symmetrized products $\psi_b(\mathbf{r}_1, \mathbf{r}_2, \dots, \mathbf{r}_N)$ of the one-particle basis functions $\underbrace{u_{n,m,n_z}}_n(\mathbf{r}) \equiv u_n(\mathbf{r})$ introduced earlier:

$$\Psi(\mathbf{r}_1, \mathbf{r}_2, \dots, \mathbf{r}_N) = \sum_b C_b \psi_b(\mathbf{r}_1, \mathbf{r}_2, \dots, \mathbf{r}_N)$$

with $\psi_b(\mathbf{r}_1, \mathbf{r}_2, \dots, \mathbf{r}_N) = \frac{1}{\sqrt{N!}} \sum_P P \left(\frac{1}{\sqrt{\nu_0!}} \prod_{i=1}^{\nu_0} u_0(\mathbf{r}_i) \cdot \frac{1}{\sqrt{\nu_1!}} \prod_{i=\nu_0+1}^{\nu_0+\nu_1} u_1(\mathbf{r}_i) \cdots \right. \right. \frac{1}{\sqrt{\nu_k!}} \left. \left. \prod_{i=\nu_0+\nu_1+\cdots+\nu_{k-1}+1}^{\nu_0+\nu_1+\cdots+\nu_{k-1}+\nu_k} u_k(\mathbf{r}_i) \right) \right),$

$$b \equiv (\nu_0, \nu_1, \dots, \nu_j, \dots, \nu_k), \quad \sum_{j=0}^k \nu_j = N, \quad \sum_{j=0}^k \nu_j m_j = L_z.$$

Here $\{C_b\}$ are the variational parameters, and P permutes the N particle co-ordinates. Also, ν_j is the occupancy of the j th single-particle basis function(u_j). The many-body quantum index b , labelling the many-body basis function $\psi_b(\mathbf{r}_1, \dots, \mathbf{r}_N)$, stands for a set of single-particle quantum numbers required to satisfy the above two defining relations between the single-particle occupation quantum numbers $\{\nu_j\}$, the single-particle angular momentum quantum numbers $\{m_j\}$, the number of particles N and the total angular momentum L_z . At this point it becomes more convenient to switch over to second-quantization notation in the occupation number (ν_j) representation. The basis function is then

$$|\psi_b\rangle \equiv \frac{\left(a_0^\dagger\right)^{\nu_0} \left(a_1^\dagger\right)^{\nu_1} \left(a_2^\dagger\right)^{\nu_2} \cdots \left(a_k^\dagger\right)^{\nu_k}}{\sqrt{\nu_0! \nu_1! \nu_2! \cdots \nu_k!}} |0\rangle \quad \text{with} \quad \sum_{j=0}^k \nu_j = N, \quad \sum_{j=0}^k \nu_j m_j = L_z$$

$$\equiv \left| (\nu_0 \nu_1 \cdots \nu_k) : \sum_{j=0}^k \nu_j = N, \sum_{j=0}^k \nu_j m_j = L_z \right\rangle, \quad (7)$$

and the many-body Hamiltonian written in the second-quantized notation is

$$\mathbf{H} = \sum_{\mathbf{i}, \mathbf{j}} \langle \mathbf{i} | 1 | \mathbf{j} \rangle a_{\mathbf{i}}^\dagger a_{\mathbf{j}} + \frac{1}{2} \sum_{\mathbf{i}_1, \mathbf{j}_1} \sum_{\mathbf{i}_2, \mathbf{j}_2} \langle \mathbf{i}_1, \mathbf{i}_2 | 2 | \mathbf{j}_1, \mathbf{j}_2 \rangle \left(a_{\mathbf{i}_1}^\dagger a_{\mathbf{j}_1} a_{\mathbf{i}_2}^\dagger a_{\mathbf{j}_2} - \delta_{\mathbf{i}_1 \mathbf{j}_1} a_{\mathbf{i}_1}^\dagger a_{\mathbf{j}_2} \right)$$

Here $a_{\mathbf{j}}^\dagger (a_{\mathbf{j}})$ are the usual bosonic creation(annihilation) operators, and $\langle \mathbf{i} | 1 | \mathbf{j} \rangle$ and $\langle \mathbf{i}_1, \mathbf{i}_2 | 2 | \mathbf{j}_1, \mathbf{j}_2 \rangle$ are the one-body and the two-body matrix-elements respectively over the single-particle basis functions. The evaluation of matrix-elements for the kinetic energy and the harmonic trapping potential over the single-particle basis chosen in the previous section is trivial. It is also possible to obtain closed form expressions for the matrix-elements for the two-body (as also for the n -body, $n=2,3,\dots$) gaussian potential(s) over the above basis as they reduce to multi-dimensional gaussian integrals. (In the calculations presented here, however, we have not considered the three or the higher-body potentials).

The variational parameters $\{C_b^0\}$ for the ground state wavefunction $\Psi_0 = \sum_b C_b^0 \psi_b$ are now determined by minimizing $K_0 \{\Psi_0\} \equiv \langle \Psi_0 | \mathbf{H} | \Psi_0 \rangle - E_0 \langle \Psi_0 | \Psi_0 \rangle$ with respect to Ψ_0 . The Lagrange multiplier E_0 is identified as the

variational energy for the ground state. The i th excited state $\Psi_i = \sum_b C_b^i \psi_b$ is determined by carrying out the variational minimization in the restricted Hilbert subspace which is orthogonal to the $(i-1)$ states determined earlier, i.e. by minimizing $K_i \{ \Psi_i \} \equiv \langle \Psi_i | \mathbf{H} | \Psi_i \rangle - E_i \langle \Psi_i | \Psi_i \rangle$ with $\langle \Psi_j | \Psi_i \rangle = 0$ for $j = 0, 1, \dots, (i-1)$.

The Davidson algorithm of iterative diagonalization¹⁸ is based on a procedure where one keeps a minimum set of i orthogonal, trial wavefunctions which spans a small subspace \mathcal{S}_i of the full many-body Hilbert space:

$$\mathcal{S}_i \equiv \left\{ \Psi_j \mid \Psi_j = \sum_b C_b^j \psi_b, \quad j = 0, 1, \dots, i \quad \text{and} \quad \langle \Psi_j | \Psi_k \rangle = \delta_{jk} \quad \text{for} \quad j, k = 0, 1, \dots, i \right\}.$$

This small subspace \mathcal{S}_i is chosen to contain dominant contributions from the ground state and the first few excited states. An $i \times i$ representation $H^{(i)}$ of the Hamiltonian \mathbf{H} is obtained over this small subspace to set up the small eigenvalue equation $H^{(i)} \mathbf{a}_\nu = \lambda_\nu^i \mathbf{a}_\nu$, $\nu = 0, 1, 2, \dots, i$. $H^{(i)}$ is an effective Hamiltonian for the system over the small subspace \mathcal{S}_i spanned by $\{ \Psi_j, \quad j = 0, 1, 2, \dots, i \}$. The eigenvalue λ_ν^i is the ν th approximate eigenvalue. The convergence for the ν th state is achieved when the residual vector for the ν th state $|\Delta\Psi_\nu\rangle = \mathbf{H}|\Psi_\nu\rangle - \lambda_\nu^i|\Psi_\nu\rangle$ becomes a null vector. If the convergence has not been achieved, the residual vector $\Delta\Psi_\nu$, after orthonormalization, is added to the list of trial vectors to augment the subspace \mathcal{S}_i to obtain $\mathcal{S}_{i+1} = \{ \Psi_j, \quad j = 0, 1, 2, \dots, i+1 \}$. The procedure is continued till the convergence is obtained. In the process, if the size of the subspace \mathcal{S}_i becomes unwieldingly large, a certain number of higher eigenvectors are dropped from \mathcal{S}_i and the procedure once again initiated.

For $N=15$ particles, for example, we have carried out calculations for all the total angular momentum states in the regime $0 \leq L_z \leq 3N$. Diagonalization of the Hamiltonian matrix is performed for each of the subspaces of L_z separately. (We have set $n_z = 0$ in the single-particle basis function $u_{n_z}(z)$ as discussed earlier.) The single-particle basis $u_{n,m}(r_\perp, \phi)$ with $n \equiv 2n_r + |m|$ and $n_r = 0, 1, \dots$, & $|m| = 0, 1, 2, \dots$, spanning the 2D x-y plane for a given subspace of L_z , is chosen as follows. It is convenient to define $l \equiv \left[\frac{L_z}{N} \right]$, where for real x , the symbol $[x]$ denotes the greatest integer less than or equal to x . For very weakly interacting particles, almost all the particles will condense into a single one-particle state, $n = m = l$, a Yrast-like state. As the interaction becomes stronger, the particles start scattering out to other single-particle states around this state, i.e. some of the particles go to states with higher angular momentum while some of them go to states with lower angular momentum (the two-body interaction conserves the total angular momentum). The single-particle angular momentum for the basis functions is now chosen to be: $m = l - n_b, l - n_b + 1, \dots, l + n_b - 1, l + n_b$, where n_b is some positive integer that we have chosen to be 3, 4 or more depending on the strength of the interaction and the computational resources available (n_b is a kind of the size of the single-particle basis chosen for the calculation for a given value of L_z and describes configurational interaction). In all our calculations presented here we have taken $n_r = 0, 1$, and $n_b = 3$. Thus for example, for $N=15$ and for the chosen subspace $L_z = 33$, we get $l \equiv \left[\frac{L_z}{N} \right] = 2$, and the single-particle angular momentum quantum number takes values $m = -1, 0, +1, +2, +3, +4, +5$. Then, with $n_r = 0, 1$, the single-particle basis set turns out to be

$$\{u_{0,0}, \quad u_{1,+1}, \quad u_{2,+2}, \quad u_{3,+3}, \quad u_{4,+4}, \quad u_{5,+5}, \quad u_{1,-1}, \quad u_{2,0}, \quad u_{3,+1}, \quad u_{4,+2}, \quad u_{5,+3}, \quad u_{3,-1}\}.$$

Thus, the $N(=15)$ -body basis functions $\{\psi_b\}$, for the $L_z = 33$ subspace, are to be constructed from these single-particle basis functions. These were used in turn to construct the variational trial function $\Psi = \sum_b C_b \psi_b$, and hence the ground state properties for the given value of L_z .

IV. CRITICAL ANGULAR VELOCITIES AND DENSITY PROFILES FOR THE CONFINED ROTATING BOSE GAS AT ZERO TEMPERATURE

From the variational ground state wavefunction $\Psi_0(\mathbf{r}_1, \dots, \mathbf{r}_N)$ obtained in the previous section, we now, in the following, go on to calculate various quantities of interest.

Let us first calculate the critical angular velocities $\{\Omega_{ci}\}$ for the onset of different vortical states. Note that for the system of N particles confined in a trap rotating at an angular velocity Ω , the thermodynamic equilibrium corresponds to the minimum of the free energy F given by $\exp\{-\beta F\} = \text{Tr} \left(\exp \left\{ -\beta \left(\hat{\mathbf{H}}^{lab} - \hbar\Omega \hat{\mathbf{L}}_z^{lab} \right) \right\} \right)$, where $\hat{\mathbf{H}}^{lab} - \hbar\Omega \hat{\mathbf{L}}_z^{lab} \equiv \hat{\mathbf{H}}^{rot}(\Omega)$, as we have noted earlier, is the Hamiltonian of the system in the co-rotating frame. For a system at $T=0$, the expression for the free energy reduces to a more simpler form $F = \langle \Psi_0 | \left(\hat{\mathbf{H}}^{lab} - \hbar\Omega \hat{\mathbf{L}}_z^{lab} \right) | \Psi_0 \rangle = \langle \hat{\mathbf{H}}^{lab} \rangle - \hbar\Omega \langle \hat{\mathbf{L}}_z^{lab} \rangle$ where Ψ_0 is the ground state wavefunction of the system in the laboratory frame for a given value of L_z obtained, in our case, variationally. The above relation can as well be seen as the minimization of the energy $\langle \hat{\mathbf{H}}^{lab} \rangle \equiv E_0^{lab}$

subject to the constraint that the system has the angular momentum expectation value $\langle \hat{\mathbf{L}}_z^{lab} \rangle$. The angular velocity Ω is then the corresponding Lagrange multiplier. Since we have constructed our variational wavefunction Ψ_0 to be an eigenfunction of the total angular momentum operator $\hat{\mathbf{L}}_z^{lab}$, we will necessarily have $\langle \hat{\mathbf{L}}_z^{lab} \rangle = \mathbf{L}_z$. Initially, when the system is subjected to no external rotation, the angular momentum state $\mathbf{L}_z = 0$ corresponds to the ground state of the system. As the system is rotated, other non-zero angular momentum states ($\mathbf{L}_z \neq 0$) successively become the ground state of the system. These are obtained by minimizing the energy $E_0^{rot}(\mathbf{L}_z, \Omega, \Lambda_2)$ in the rotating frame:

$$E_0^{rot}(\mathbf{L}_z, \Omega, \Lambda_2) \equiv E_0^{lab}(\mathbf{L}_z, \Lambda_2) - \hbar \Omega \mathbf{L}_z^{lab} \quad (8)$$

Here Λ_2 measures the two-body interaction strength and has been defined in an earlier section. Thus, the critical angular velocity Ω_c beyond which the higher angular momentum state \mathbf{L}_z , say, becomes lower in energy in the rotating frame compared to the lower angular momentum state \mathbf{L}'_z ($< \mathbf{L}_z$) is given by:

$$\Omega_c = \frac{E_0^{lab}(\mathbf{L}_z, \Lambda_2) - E_0^{lab}(\mathbf{L}'_z, \Lambda_2)}{(\mathbf{L}_z - \mathbf{L}'_z) \hbar} \quad (9)$$

This gives us a number of critical angular velocities $\{\Omega_{ci}, i = 0, 1, 2, \dots\}$ at which the ground state of the rotating system changes its angular momentum state abruptly. The angular momentum \mathbf{L}_z of the ground state *vs* the angular velocity Ω relation, called the $\mathbf{L}_z - \Omega$ -phase diagram, or the stability line, for the rotating system was calculated in terms of the variational ground states obtained. We present this in Fig. 1.

Next, we calculate the density profile and the circulation for the vortex states. For this we need the single-particle reduced density-matrix. From the many-body ground state wavefunction $\Psi_0(\mathbf{r}_1, \dots, \mathbf{r}_N)$, obtained through the variational exact diagonalization(ED), the one-particle reduced density matrix $\rho_1(\mathbf{r}, \mathbf{r}')$ is obtained by integrating out the N-1 co-ordinates:

$$\begin{aligned} \rho_1(\mathbf{r}, \mathbf{r}') &\equiv \int \int \dots \int d\mathbf{r}_2 \mathbf{r}_3 \dots \mathbf{r}_N \Psi_0^*(\mathbf{r}, \mathbf{r}_2, \mathbf{r}_2, \dots, \mathbf{r}_N) \Psi_0(\mathbf{r}', \mathbf{r}_2, \mathbf{r}_3, \dots, \mathbf{r}_N) \\ &= \sum_n \sum_m \sum_{n_z} \sum_{n'} \sum_{m'} \sum_{n'_z} \rho_{nmn_z, n'm'n'_z} u_{n,m,n_z}^*(\mathbf{r}) u_{n',m',n'_z}(\mathbf{r}') \\ &\equiv \sum_{\mu} \lambda_{\mu} \chi_{\mu}^*(\mathbf{r}) \chi_{\mu}(\mathbf{r}'), \\ \text{with } \chi_{\mu}(\mathbf{r}) &\equiv \sum_n \sum_m \sum_{n_z} c_{n,m,n_z}^{\mu} u_{n,m,n_z}(\mathbf{r}) \quad \text{and} \quad \sum_{\mu} \lambda_{\mu} = 1, \end{aligned} \quad (10)$$

where $\{\lambda_{\mu}\}$ are the eigenvalues and $\{\chi_{\mu}(\mathbf{r})\}$ the corresponding eigenvectors of the one-particle reduced density-matrix $\rho_1(\mathbf{r}, \mathbf{r}')$. The diagonal part $\rho_1(\mathbf{r}, \mathbf{r}) \equiv \rho(\mathbf{r})$ gives the single-particle density-profile of the system(the condensate + the non-rotating fraction + the above-the-condensate fraction). For our finite system, the BEC corresponds to a single eigenvalue λ_{μ} being significantly larger than the rest of the eigenvalues. As noted before, our system is quasi-2D, *i.e.*, there is practically no excitation in the z-direction. So we take $n_z = 0$ and the summation over n_z goes off. Also, we note that $\chi_{\mu}(\mathbf{r})$ is an eigenvector of the single-particle angular momentum $\hat{\mathbf{L}}_z$ with eigenvalue m_{μ} , hence the summation over m in equation(10) too goes away. The only summation that we are left with is then over n_{μ} ($\equiv 2n_{r\mu} + |m_{\mu}|$, where $n_{r\mu} = 0, 1, 2, \dots$). Thus we get

$$\chi_{\mu}(\mathbf{r}) = \sum_{n_{\mu}=|m_{\mu}|, |m_{\mu}|+2, \dots} c_{n_{\mu}, m_{\mu}, 0}^{\mu} u_{n_{\mu}, m_{\mu}, 0}(\mathbf{r}) \quad (11)$$

Note that n_{μ} increases in steps of 2, which comes from quantization. Tracing out the z co-ordinate, the density $\rho(r_{\perp}, \phi)$, the current $j_{\phi}(r_{\perp}, \phi)$, the velocity $v_{\phi}(r_{\perp}, \phi)$ and the circulation $\kappa(r_{\perp})$ profiles in the x-y plane, for the quasi-2D system, turn out to be

$$\begin{aligned} \rho(r_{\perp}, \phi) &= \frac{\alpha_{\perp}^2}{\pi} \cdot e^{-\alpha_{\perp}^2 r_{\perp}^2} \sum_{\mu} \lambda_{\mu} \\ &\left| \sum_{n_{\mu}=|m_{\mu}|, |m_{\mu}|+2, \dots} c_{n_{\mu}, m_{\mu}, 0}^{\mu} \sqrt{\frac{(\frac{1}{2}[n_{\mu} - |m_{\mu}|])!}{(\frac{1}{2}[n_{\mu} + |m_{\mu}|])!}} (r_{\perp} \alpha_{\perp})^{|m_{\mu}|} L_{\frac{1}{2}(n_{\mu} - |m_{\mu}|)}^{|m_{\mu}|} (r_{\perp}^2 \alpha_{\perp}^2)^{\frac{1}{2}} \right|^2 \end{aligned}$$

$$\equiv \rho(r_\perp), \quad (12)$$

$$j_\phi(r_\perp, \phi) = \sqrt{\frac{\hbar\omega_\perp}{m}} \cdot \left(\frac{1}{\alpha_\perp r_\perp}\right) \cdot \sum_\mu m_\mu \lambda_\mu |\chi_\mu(r_\perp, \phi)|^2 \equiv j_\phi(r_\perp), \quad (13)$$

$$\text{and } j_{r_\perp}(r_\perp, \phi) = j_z(r_\perp, \phi) = 0;$$

$$v_\phi(r_\perp, \phi) = \sqrt{\frac{\hbar\omega_\perp}{m}} \cdot \left(\frac{1}{\alpha_\perp r_\perp}\right) \cdot \sum_\mu m_\mu \lambda_\mu \frac{|\chi_\mu(r_\perp, \phi)|^2}{\rho(r_\perp, \phi)} \equiv v_\phi(r_\perp), \quad (14)$$

$$\text{and } v_{r_\perp}(r_\perp, \phi) = v_z(r_\perp, \phi) = 0;$$

$$\begin{aligned} \kappa(r_\perp) &\equiv \oint_{r_\perp=\text{constant}} \mathbf{v} \cdot d\mathbf{l} = \int_0^{2\pi} v_\phi(r_\perp) r_\perp d\phi = 2\pi r_\perp v_\phi(r_\perp) \\ &= 2\pi \frac{\hbar}{m} \sum_\mu m_\mu \lambda_\mu \frac{|\chi_\mu(r_\perp, \phi)|^2}{\rho(r_\perp, \phi)}. \end{aligned} \quad (15)$$

These are plotted in Figs. 2-4. For completeness we also give the velocity curl

$$\begin{aligned} \nabla \times \mathbf{v} &= \frac{\hat{z} \omega_\perp}{\rho(r_\perp, \phi)} \sum_\mu \lambda_\mu \left(\frac{m_\mu}{r_\perp \alpha_\perp} - v_\phi \sqrt{\frac{m}{\hbar\omega_\perp}} \right) \left[\chi_\mu^* \left(\sum_{n_\mu} c_{n_\mu, m_\mu, 0} \right. \right. \\ &\quad \left. \left. \left\{ n_\mu u_{n_\mu, m_\mu, 0} - \sqrt{(n_\mu - |m_\mu|)(n_\mu + |m_\mu|)} u_{n_\mu - 2, m_\mu, 0} \right\} \right) + c.c \right]. \end{aligned} \quad (16)$$

The expression for circulation as in equation(15) calls for some discussion. The circulation associated with each of the eigencomponents(χ_μ) of the one-particle density-matrix is, of course, quantized as integral multiples of $\frac{\hbar}{m}$ for any closed path, and clearly can have no r_\perp dependence for the circular paths chosen for our line integral. The expression in equation(15), however, involves an average over different components χ_μ , and can, therefore, assume non-integral values that vary with r_\perp for the chosen circular path $r_\perp=\text{constant}$. This reflects the radial variation of the relative fractional weights $m_\mu \lambda_\mu |\chi_\mu(r_\perp, \phi)|^2$ of the different fractions with r_\perp .

V. RESULTS AND DISCUSSION

The results and discussions given below refer to the following choice of parameters: $a_\perp = 1.222\mu\text{m}$, $\lambda_z = \sqrt{8}$, $a_{sc} = 1000a_0$, where a_0 is the Bohr radius. Please note that the scattering length a_{sc} chosen above is 10 times more than as given in¹⁹ for ⁸⁷Rb. Further, we present here the results for N=15 only in the angular momentum regime $0 \leq L_z \leq 3N$. We have, however, done the calculations for N=6 and N=10 also. First we note that we are always in the dilute gas limit here inasmuch as $N \left(\frac{a_{sc}}{a_{ho}} \right)^3 \ll 1$, with $a_{ho} \equiv (a_\perp^2 a_z)^{\frac{1}{3}} = a_\perp \lambda_z^{-\frac{1}{6}}$. Further, we are also in the regime of moderate ($a_{sc} = 1000a_0$) to very weak($a_{sc} = 1a_0$) interaction strength as the parameter $N \frac{a_{sc}}{a_{ho}}$ is of order 1 or much much less than 1 for the two regimes respectively. Moreover for $a_{sc} = 1000a_0$, the healing length $\xi (\equiv (8\pi n a_{sc})^{-\frac{1}{2}}$, with $n \sim \frac{N}{a_{ho}^3}$, the mean particle density) < the oscillator length $a_{ho} \sim$ the size of the system. Thus our study for the above choice of parameters may be relevant to bulk systems.

The critical angular velocity Ω_{c1} for the single-vortex state($L_z = N$) decreases for increasing value of N. Thus for $a_{sc} = 1000a_0$, it is $0.88487\omega_\perp$ and $0.84493\omega_\perp$ for N=10 and 15 respectively. For a given N, the critical angular velocity Ω_{c1} is also found to decrease with increasing scattering length a_{sc} . Thus for N=15, Ω_{c1} (in units of ω_\perp) are found to be .99978, .99783, 0.97901 and 0.84493 for $a_{sc} = 1a_0$, $10a_0$, $100a_0$, $1000a_0$ respectively. The condensate fraction for a given N and corresponding to one of the stable vortex states, however, seems to be quite insensitive to a change in the scattering length. Thus for $L_z=N=15$ state and $a_{sc} = 1a_0$, $10a_0$, $100a_0$, $1000a_0$, the condensate fractions(λ_1) are found to be 0.87826767, 0.87822606, 0.87777931, 0.87069438 respectively.

In Table 1, we summarize our results for the ground state of the N=15 system in different subspaces of the total angular momentum L_z in the regime $0 \leq L_z \leq 3N$ for $a_{sc} = 1000a_0$. As the system is rotated, a number of (total) angular momentum states are found to be stable at successively higher angular velocities Ω_{ci} , $i = 1, 2, \dots$. We have also given the density-matrix eigenvalues(λ_μ) and the corresponding single-particle angular momentum quantum number(m_μ) for the largest three fractions($\lambda_1 > \lambda_2 > \lambda_3$). We note that, corresponding to each of the stable ground states of the rotating system, namely, $L_z = 15, 26, 30, 33, 35, 36, 45, \dots$ for N=15, the second largest fraction is

found to be non-rotating, *i.e.* $m_2 = 0$. The single-particle angular momentum quantum number m_1 , corresponding to the largest fraction, is taken to be the vorticity of the condensate.

Figure 1 gives the $L_z - \Omega$ phase diagram, or the stability line. One can readily identify the successive critical angular velocities $\{\Omega_{ci}, i = 0, 1, 2, \dots\}$ for the transition from one stable state to another stable state. Several points are to be noted here. The non-integral values for the angular momentum per particle clearly indicates the incomplete condensation, *i.e.*, the fact that more than one eigenvalues $\{\lambda_\mu\}$ of the reduced density-matrix are non-zero. This is, however, not to be taken as the fragmented condensate²⁰, but merely as depletion of the condensate/superfluid fraction due to the interaction and the rotation. Also, we have observed that the critical angular velocity Ω_{ci} decreases monotonically with increasing repulsive interaction and the particle number. This can be readily understood physically from the expression in equation(9) for the critical angular velocity $\Omega_{ci}(L_z)$ if one remembers that the non-rotating ($L_z = 0$ angular momentum) state is more compact and, therefore, has its energy raised (because of the repulsive interaction) relative to the expanded higher angular momentum states. More importantly, however, our critical angular velocity Ω_{ci} for a given N , is systematically greater than the non-variational value based on the Yrast-like state^{14,15,12,13}. We expect this to be due to our more accurate and, therefore, lower variational ground state energies.

In Fig.(2a) we have plotted the total (the condensate+the non-rotating component+the above-the-condensate fraction) density profile $\rho(r_\perp)$ for the $L_z=N$ single-vortex angular momentum state of the system. We have also plotted separately the density profiles for the condensate fraction $\lambda_1 |\chi_1(\mathbf{r})|^2$ corresponding to the largest eigenvalue $\lambda_1 (= 0.87069)$ in Fig.(2b), the non-rotating component $\lambda_2 |\chi_2(\mathbf{r})|^2$ corresponding to the second largest eigenvalue $\lambda_2 (= 0.06576)$ in Fig.(2c), and the above-the-condensate fraction in Fig.(2d) corresponding to the remaining components of the one-particle reduced density matrix:

$$\rho(\mathbf{r}, \mathbf{r}') = \underbrace{\lambda_1 \chi_1^*(\mathbf{r}) \chi_1(\mathbf{r}')}_{\text{the condensate with } m_1 = 1} + \underbrace{\lambda_2 \chi_2^*(\mathbf{r}) \chi_2(\mathbf{r}')}_{\text{the non-rotating component with } m_2 = 0} + \underbrace{\sum_{\mu=3} \lambda_\mu \chi_\mu^*(\mathbf{r}) \chi_\mu(\mathbf{r}')}_{\text{the above-the-condensate}}$$

where, as we have earlier, m_μ is the single-particle angular momentum quantum number associated with the μ th component of the density-matrix. As we go to higher Ω , the condensate depletes—with the non-rotating component and the above-the-condensate fractions becoming more pronounced(as can also be seen from Table 1).

Figure 3 depicts the velocity profile for the total system(3a), for the condensate(3b), for the non-rotating component(3c), and for the above-the-condensate fractions(3d) respectively.

Figure 4 depicts the circulation profile for circular paths of radii r_\perp in the x-y plane: (4a) for the total system, (4b) for the condensate fraction, (4c) for the non-rotating fraction, and (4d) for the above-the-condensate fraction respectively. As can readily be seen, the condensate fraction has an integral circulation and is constant over space, while the total as well as the above-the-condensate fraction has non-integral circulation and varies with r_\perp as explained earlier below equation(15).

In conclusion, our many-body variational calculation for an admittedly finite number ($N \leq 15$) of particles explicitly resolves the structure of the rotating BEC at $T=0$ in terms of the various components of the reduced one-particle density-matrix. Further work is in progress to consider spin-1 Bose particles, where we expect qualitative changes in the structure of the rotating BEC. In particular, we expect a dramatic increase in the critical angular velocities because of the spin-polarization drag effect inasmuch as the angular momentum may be absorbed preferentially in the spin rather than the orbital degrees of freedom without costing kinetic energy. This could lead to spin polarization due to rotation of the trap^{21,22}. We expect this effect to be more pronounced here than in a classical rotating system.

ACKNOWLEDGMENT

One of us(MAHA) would like to thank Prof. R. Nityananda and Prof. R. Srinivasan for useful discussions.

¹ M. H. Anderson, J. R. Ensher, M. R. Matthews, C. E. Wieman, and E. A. Cornell, Science **269**, 198 (1995).

² K. B. Davis, M.-O. Mewes, M. R. Andrews, N. J. van Druten, D. S. Durfee, D. M. Kurn, and W. Ketterle, Phys. Rev. Lett. **75**, 3969 (1995).

³ C. C. Bradley, C. A. Sackett, J. J. Tollett, and R. G. Hulet, Phys. Rev. Lett. **75**, 1687 (1995).

⁴ D. G. Fried, T. C. Killian, L. Willmann, D. Landhuis, S. C. Moss, D. Kleppner, and T. J. Gretyak, Phys. Rev. Lett. **81**, 3811 (1998).

⁵ G. Baym and C. J. Pethick, Phys. Rev. Lett. **76**, 6 (1996).

⁶ F. Dalfovo, S. Giorgini, L. P. Pitaevskii, and S. Stringari, Rev. Mod. Phys. **71**, 463 (1999).

⁷ See, Proceedings of the International School of Physics “Enrico Fermi”, Course CXL, Edited by M. Inguscio, S. Stringari, and C. E. Wieman, (IOS Press, Netherlands) 1999.

⁸ S. Inouye, M. R. Andrews, J. Stenger, H. -J. Miesner, D. M. Stamper-Kurn, and W. Ketterle, Nature, **392**, 151 (1998).

⁹ M. R. Matthews, B. P. Anderson, P. C. Haljan, D. S. Hall, C. E. Wieman, and E. A. Cornell, Phys. Rev. Lett. **83**, 2498 (1999).

¹⁰ K. W. Madison, F. Chevy, W. Wohleben, and J. Dalibard, Phys. Rev. Lett. **84**, 806 (2000).

¹¹ M. R. Andrews, C. G. Townsend, H.-J. Miesner, D. S. Durfee, D. M. Kurn, and W. Ketterle, Science **275**, 637 (1997).

¹² G. F. Bertsch and T Papenbrock, Phys. Rev. Lett. **83**, 5412 (1999).

¹³ N. K. Wilkin and J. M. F. Gunn, Phys. Rev. Lett. **84**, 6 (2000).

¹⁴ D. A. Butts and D. S. Rokhsar, Nature **397**, 327 (1999).

¹⁵ B. Mottelson, Phys. Rev. Lett. **83**, 2695 (1999).

¹⁶ V. Fock, Z. Physik **47**, 446 (1928).

¹⁷ C. G. Darwin, Proc. Cambridge Philos. Soc. **27**, 86 (1930).

¹⁸ E. R. Davidson, J. Comput. Phys. **17**, 87 (1975).

¹⁹ F. Dalfovo and S. Stringari, Phys. Rev. A **53**, 2477 (1996).

²⁰ P. Nozieres and D. Saint James, J. Phys.(Paris) **43**, 1133 (1982).

²¹ E. T. Jaynes, Phys. Rev. **106**, 620 (1957).

²² N. Agarwal and N. Kumar(unpublished).

Table caption

Table 1. Gives the largest three condensate fractions $\lambda_1 > \lambda_2 > \lambda_3$ and the corresponding single-particle angular momentum eigenvalues m_1, m_2 and m_3 in the one-particle reduced density-matrix for the ground state of the rotating BEC, in given subspaces of total angular momentum L_z . Also given are the ground state energies $E_0^{lab}(L_z)$ in the laboratory frame and the critical angular velocities Ω_{ci} corresponding to the stable ground states of the rotating system in the angular momentum regime $0 \leq L_z \leq 3N$.

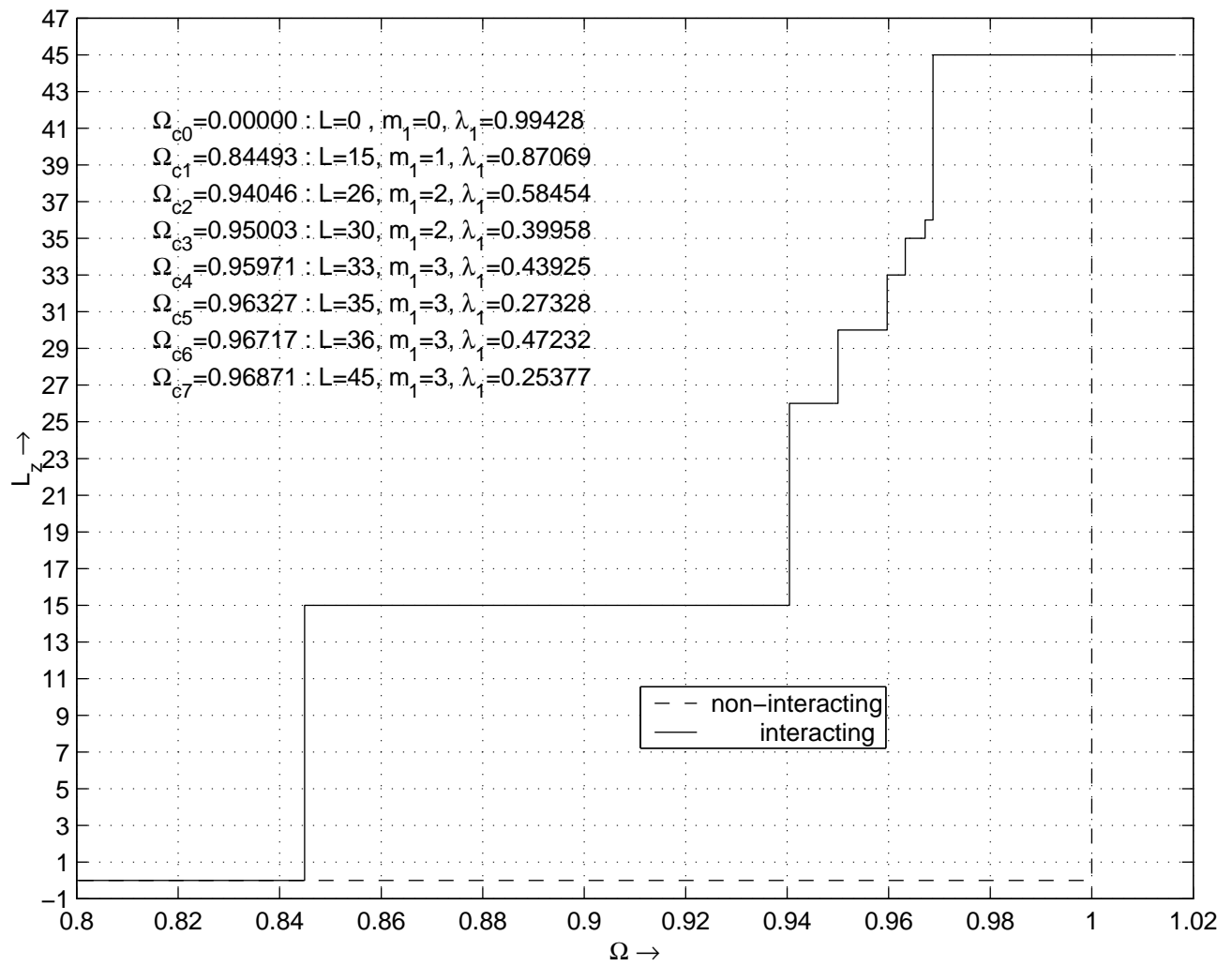
Figure captions

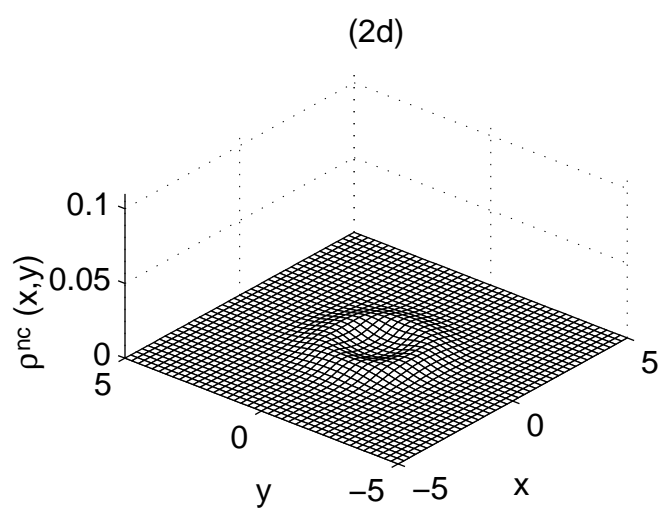
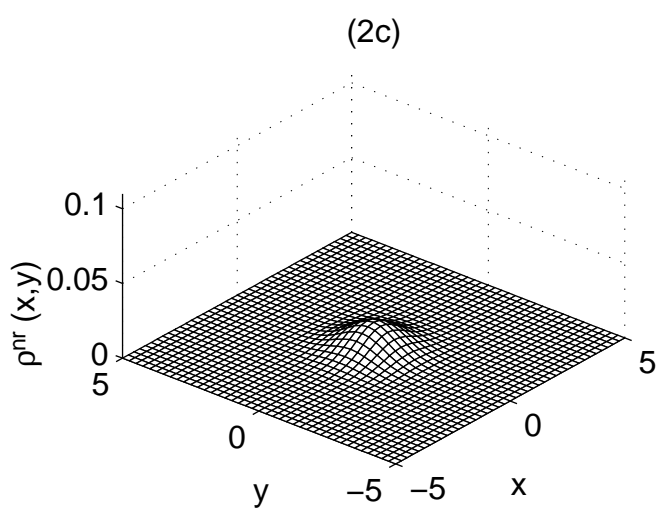
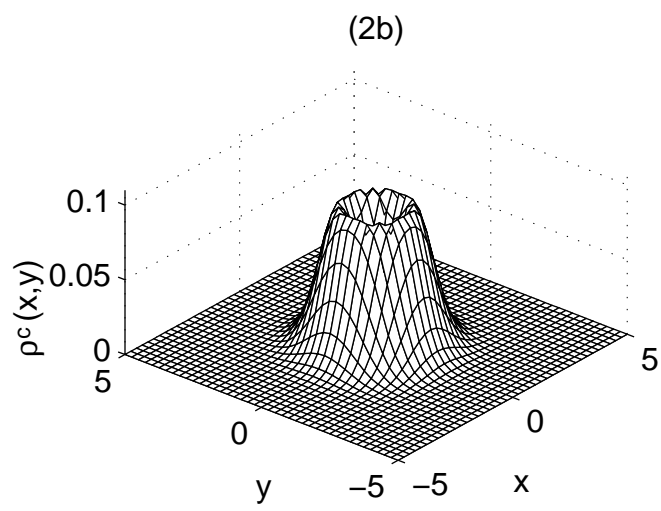
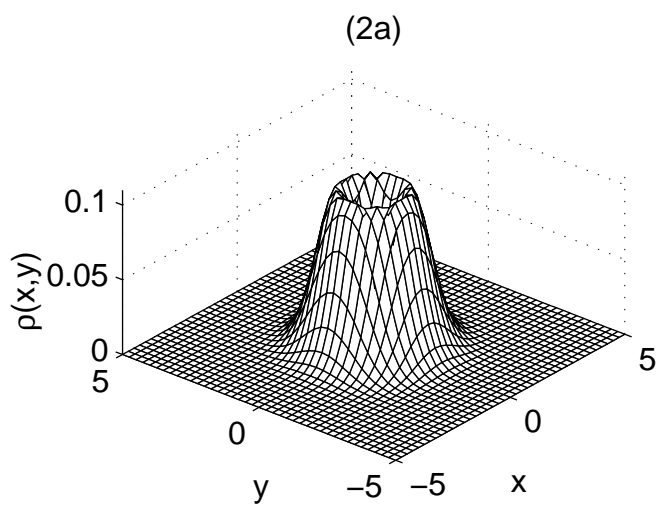
FIG.1. Gives the plot (solid line) for the total angular momentum L_z in units of \hbar *versus* the critical rotational velocity Ω_{ci} (in units of ω_\perp) for the rotating BEC. Dashed line is for the non-interacting case, included here for reference.

FIG.2. Depicts the normalized particle-density in units of a_\perp^{-2} for, (a) the total system, (b) the condensate fraction, (c) the non-rotating component, and (d) the above-the-condensate fraction, in the x-y plane. Distances are in units of a_\perp .

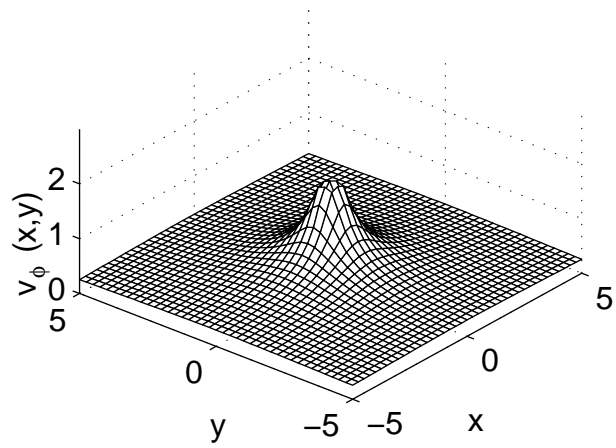
FIG.3. Depicts the azimuthal velocity profile $v_\phi(r_\perp)$ in units of $\sqrt{\frac{\hbar\omega_\perp}{m}}$ for, (a) the total system, (b) the condensate fraction, (c) the non-rotating component, and (d) the above-the-condensate fraction, in the x-y plane. Distances are in units of a_\perp .

FIG.4. Depicts the circulation $\kappa(r_\perp) \equiv \oint \mathbf{v} \cdot d\mathbf{l}$ profile in units of $\frac{\hbar}{m}$ along circular paths of radius r_\perp in the x-y plane for, (a) the total system, (b) the condensate fraction, (c) the non-rotating component, and (d) the above-the-condensate fraction. Distances are in units of a_\perp .

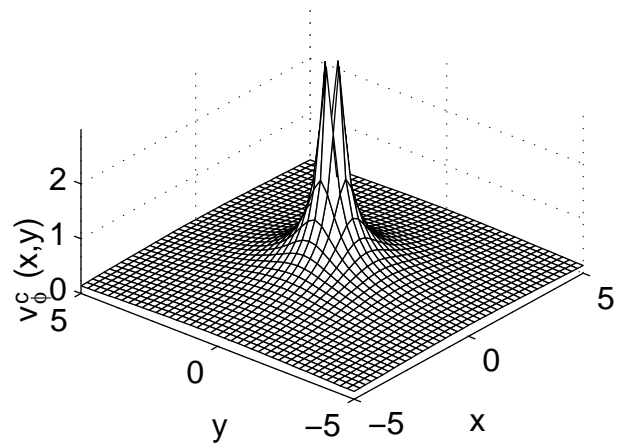




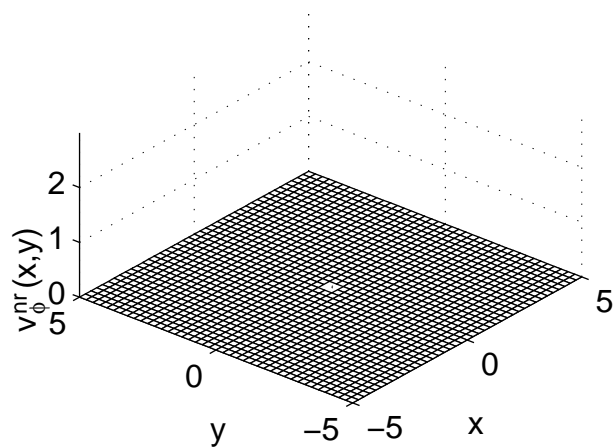
(3a)



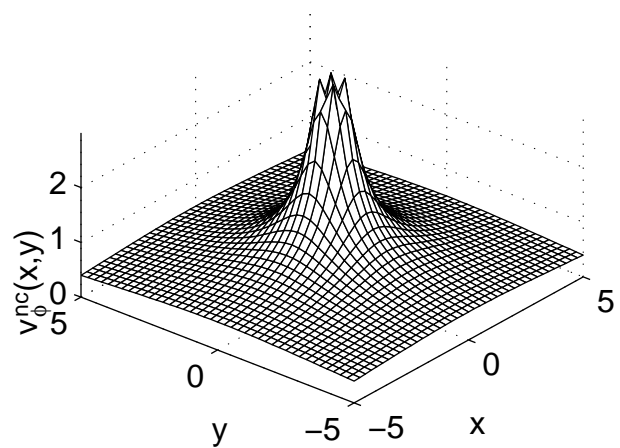
(3b)



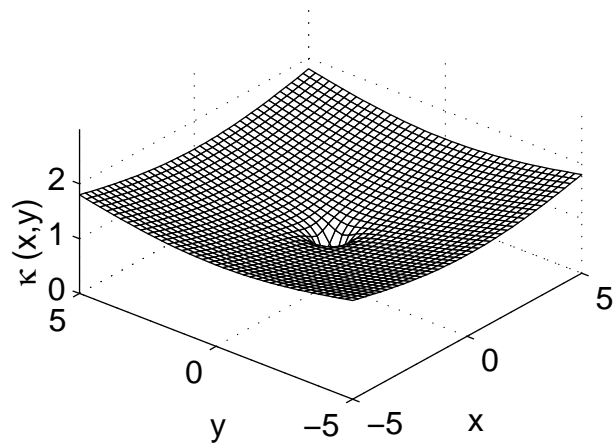
(3c)



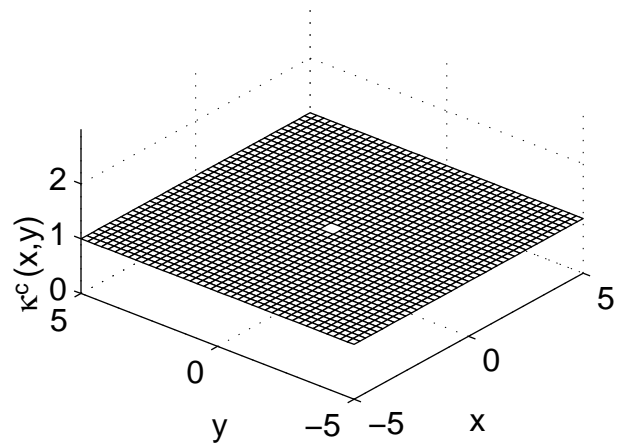
(3d)



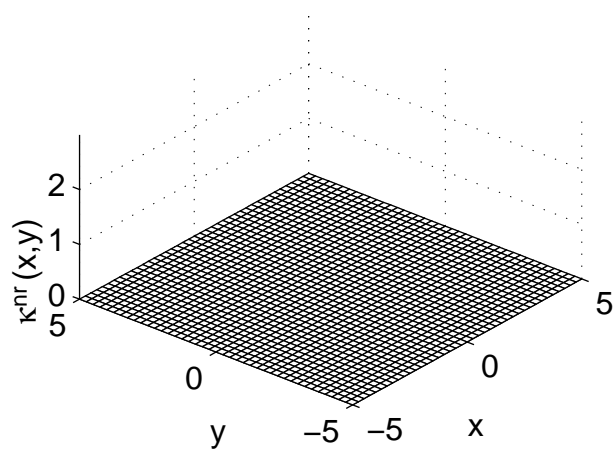
(4a)



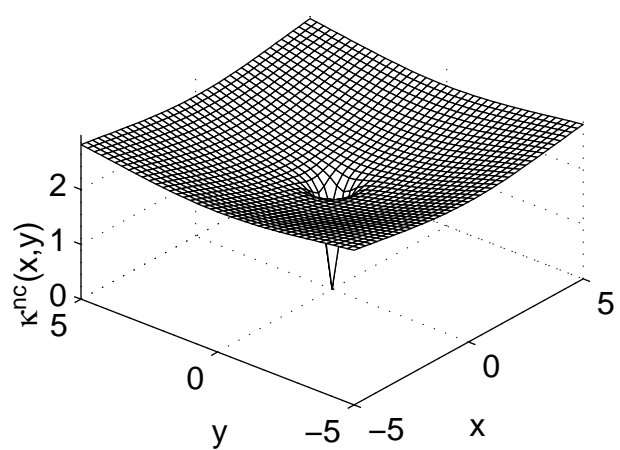
(4b)



(4c)



(4d)



		the largest three confidence fractions ($\lambda_1 > \lambda_2 > \lambda_3$)						
L_z	$E_0^{lab}(L_z)$	$\Omega_{ci}, i = 0, 1, \dots$	the largest		the 2nd largest		the 3rd largest	
			m_1	λ_1	m_2	λ_2	m_3	λ_3
0	41.18837302	0	0	0.99427949	1	0.00212506	-1	0.00212506
1	42.19021527		0	0.92512205	1	0.06925498	-1	0.00357935
2	42.99051559		0	0.91976958	2	0.05861216	1	0.01805707
3	43.79209837		0	0.91331690	3	0.05312628	1	0.01811541
4	44.73324214		0	0.82679888	1	0.09252527	2	0.05428543
5	45.55313888		0	0.81277620	2	0.07410551	1	0.07174137
6	46.38548370		0	0.79764796	3	0.07915089	1	0.07651343
7	47.25793734		0	0.69479391	1	0.17366459	2	0.09141939
8	48.08941042		0	0.65199628	1	0.20072345	2	0.10021851
9	48.92516913		0	0.58781479	1	0.26177695	2	0.10461905
10	49.75781621		0	0.51135166	1	0.33771458	2	0.11639777
11	50.58519904		0	0.43914313	1	0.41188737	2	0.11891717
12	51.41081735		1	0.50148248	0	0.35825339	2	0.11659973
13	52.23441694		1	0.60552214	0	0.27006529	2	0.10722330
14	53.05611818		1	0.72989312	0	0.17172359	2	0.08750829
15	53.86233854	0.8449310347	1	0.87069438	0	0.06576450	2	0.05736943
16	54.86286892		1	0.70721734	2	0.15671270	0	0.11971704
17	55.84557485		1	0.61433667	2	0.18372260	0	0.15433888
18	56.72500928		1	0.72037659	2	0.10862810	0	0.09845465
19	57.69445358		1	0.52978903	2	0.23482509	0	0.15927850
20	58.64083432		2	0.36833419	1	0.29367400	0	0.25410621
21	59.56022291		1	0.40836712	2	0.28385103	0	0.18795379
22	60.48085974		2	0.48759419	0	0.28457736	1	0.13030000
23	61.43733026		2	0.44095784	0	0.22721036	1	0.20019517
24	62.33084916		2	0.54527192	0	0.25669786	1	0.08045180
25	63.31524337		2	0.44984897	0	0.20416394	1	0.16769313
26	64.20738686	0.9404589382	2	0.58454211	0	0.21375604	4	0.08790990
27	65.22391160		2	0.45177009	0	0.20652176	3	0.17972105
28	66.11545941		2	0.58577373	0	0.17728482	4	0.10875007
29	67.13035728		2	0.35563338	3	0.25959961	0	0.21675739
30	68.00748962	0.9500256900	2	0.39958349	0	0.20014133	4	0.14633062
31	68.96895640		2	0.27246493	0	0.22552958	3	0.18829877
32	69.93097790		3	0.32347211	0	0.25063967	2	0.19054894
33	70.88661130	0.9597072267	3	0.43925131	0	0.25533628	2	0.11678094
34	71.86427448		3	0.23836963	0	0.22102392	2	0.21063530
35	72.81314423	0.9632664650	3	0.27328015	0	0.23042986	2	0.17011018
36	73.78030965		3	0.47231611	0	0.20855427	4	0.11600071
37	74.77086405		3	0.29197179	0	0.21784613	2	0.16076573
38	75.74022100		3	0.33264589	0	0.21931839	4	0.16484152
39	76.69427367		4	0.25008777	3	0.22721045	0	0.22519429
40	77.66435876		4	0.41484291	0	0.27578055	5	0.10808545
41	78.68052383		4	0.29409482	0	0.25786496	5	0.19155942
42	79.64666492		4	0.22564885	0	0.21502410	3	0.21125875
43	80.60355942		4	0.36638788	0	0.21594187	5	0.15538897
44	81.56135092		4	0.50408767	0	0.23405414	5	0.11009036
45	82.49865663		3	0.25376654	0	0.20933525	4	0.19800742